Journal of Applied Research and Technology

www.jart.icat.unam.mx

Journal of Applied Research and Technology 21 (2023) 713-729

Original

Comparative study of PID, PD-FLC and PID-FLC for active magnetic bearing

S. Gupta* • P. K. Biswas

National Institute of Technology, Mizoram

Received 12 09 2021; accepted 01 18 2023
Available 10 31 2023

Abstract: In this manuscript, a closed loop active magnetic bearing system (AMB) is proposed, dynamically modelled, and linearized in form of unstable transfer function. To achieve proper bearing operation, the proposed AMB system is controlled by two separate controllers, one to control the current in the electromagnet coils by forming an inner closed loop and second to stabilize the position of the suspending object at equilibrium. To maintain the position of suspending object at equilibrium, for the proposed AMB system (considering inner closed loop as unity) a conventional PID controller, a PD-fuzzy logic controller (PD-FLC) and a PID-FLC are designed. Their effectiveness on the proposed system is evaluated and compared. Later, the effect of designed controllers on the complete proposed AMB system is studied with the help of control system plots and improvement among their performances is observed. The plotted step responses and calculated transient state parameters will verify that by changing the conventional PID controller to a PID-FLC could result in 48.34% improvement in overshoot, 41.52% increment in speed of response and 32.23% increment in the relative stability.

Keywords: Active magnetic bearing (AMB), proportional-integral-derivative (PID) controller, fuzzy logic controller (FLC), PD-FLC, PID-FLC

*Corresponding author.
E-mail address: surajgupta.5591@gmail.com(S. Gupta).
Peer Review under the responsibility of Universidad Nacional Autónoma de México.

1. Introduction

These days optimum utilization of energy and reliability is becoming an uttermost parameter to design and to develop any innovative work. The rapid advancement in research has been a great motivation for researchers and scientists to modernize their work and to evolve new ideas and concepts. Active magnetic bearing (AMB) is from one of those new ideas with many advantages over the conventional bearing and Permanent Magnetic Bearing (PMB) (Schweitzer & Maslen, 2009).

Although the fundamental principle of AMB is levitation (Schweitzer, 2005) means hovering of an object made of a ferromagnetic material such that it counterbalances gravity acting on it and that counterbalancing force will be provided by the magnet, either it is electromagnet (active magnet) or, permanent magnet (Bassani 2006). Permanent magnetic bearing (PMB) and active magnetic bearing are the two main categories of magnetic bearing based on the type of magnet utilized. In PMB, the magnet used is a permanent magnet whose magnetic strength depends on the material used (Bachovchin et al., 2013). However, with active magnetic bearings, the magnet is really an electromagnet whose magnetic force can be adjusted by restricting the amount of current passing through the coils. This adds up a great advantage, to use electromagnets (active magnets) in magnetic bearing rather than a permanent magnet, like, prolonged use of permanent magnets in magnetic bearing causes a reduction in the attractive power of permanent magnets that leads to rough and unstable bearing operation, but using a suitable controller with AMB, a stable bearing operation is possible (Bachovchin et al., Post 2012).

AMB comprises an electromagnet actuator that is made of iron with copper windings around it, and that may be in shape of 'U', 'I' etc. (Mushi et al., 2012). The rotating object is of ferromagnetic material separated by a little airgap from the electromagnet, as shown in Figure 1. Calculating the force that the electromagnet exerts on a given rotor depends on the number of copper winding turns, the current flowing through the winding, the size of the core, and the air space between them (Schweitzer & Maslen, 2009).

In this day and age of modernization, conventional equipment and devices are now replacing by the modern and efficient one and to get better performance in high-speed industrial machinery, robust environment used space machinery etc. are replacing conventional bearing from AMBs (Schweitzer et al.,1994). AMBs are widely using in fast turbo compressor (Mushi et al., 2012), flywheel energy storage system (Bai et al., 2012), artificial geographical satellites (Bangcheng et al., 2011), artificial medical equipment (Hoshi et al., 2006) and so on.

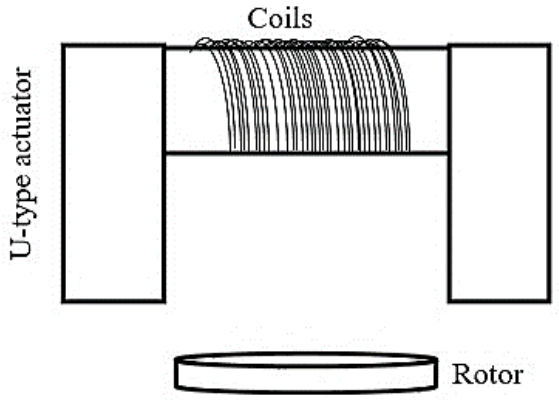

Figure 1. Single axis U-type AMB.

Controlling of nonlinear system is a prominent area of research as most of the practical system are inherently nonlinear and unstable. AMB system is one of those nonlinear system which needs a robust and efficient controller for a stable and effective performance. Various articles and research have been proposed for controlling of an AMB system, some of them are based on conventional controlling methods, like, Qing-Guo Wang et al. (1999) developed a method based on controlling of a second-order closed loop system with a pole allocation strategy to tune PID controller. In 2005, Polajzer et al. proposed a cascade connected PI and PD position controllers for decentralized control of an AMB system (Polajžer et al., 2006). Later, Imari and Yamamoto (2012) proposed a newly PID control method for nonlinear system which studied by Anantachaisilp & Lin (2013) for PID tuning of AMB system. Apart from conventional controllers, fuzzy logic-based intelligent controllers have shown to be highly successful at controlling nonlinear systems (such as AMB) as Hung (1995) in his work used a fuzzy logic to control magnetic bearing. Later, Hong & Langari, (2000) proposed a robust fuzzy control for AMB system to overcome the harmonic disturbances issue (Hong & Langari, 2000) and Du et al. (2010) developed a robust Takagi-Sugeno model based fuzzy control to stabilize the AMB with fast response speed subject to control-voltage saturation (Du et al., 2010). Further, Zhang et al. (2014) presented a fuzzy PID control logic with adjustable membership function and Raj and Mohan (2020) proposed a fuzzy PID controller with multiple fuzzy sets. Proper designing and implementation of intelligent controller can result in an improved performance of AMB system as compared to conventional controllers. This improvement in the performance is needed to be observed and analysed. Therefore, in this work, for the proposed AMB system (when inner closed loop is unity) first, a conventional PID, a PD-fuzzy

logic controller and a PID-FLC is designed and then their performance is observed. Later, these designed controllers are implemented with the complete proposed AMB system and their capability to handle system instabilities are analysed and their performances are compared.

The next portion of the study discusses the dynamical modelling of the proposed active magnetic bearing (AMB) system. The controllers' design is the main topic of Section 3. Section 4 presents all the simulations that have been conducted in MATLAB 2015b for the verification of the designed controllers with proposed system and performance comparison among them. Section 5 consists of concluding remarks.

2. Dynamical modelling of proposed closed loop active magnetic bearing (AMB) system

In Active magnetic bearing, there is no friction between the actuator and rotor and this advantage makes AMB reach at a very high speed allowed by the tear and strain of the material from which it is designed. Irrespective of the environment and location AMB performance is always better than the conventional bearing (Schweitzer & Maslen, 2009). For the proposed AMB system as shown in Figure 2. For proper and reliable bearing operation two controllers are required. One controller is in inner closed loop to control the current going to coil of the electromagnet before power amplifier and second to control position of the rotor by comparing its actual position with the reference position.

The inner closed loop of Figure 2 has a current controller which is a PI controller (Yordanova, 2009) for increase the response of current controlled inner closed loop (He et al., 2020). For power amplifier (Jiang et al., 2020), various research has been carried out and depending upon the objective of the applications power amplifier (Debnath et al., 2018) get modified. The output of the position controller compares the signal that the current sensor produces based on the amount of current flowing through the electromagnet coils. The inner closed loop acts faster (i.e., inner closed loop requires enough current loop bandwidth) as compared to the outer loop (He et al., 2020).

The outer loop is for controlling the position of rotor (suspending object) and this loop has position sensor, position controller and AMB system. The most practical step before developing and implementing the controller for the proposed AMB system is to dynamic modelling of the system (Debnath & Biswas, 2020). The model is solely used for dynamic analysis and to comprehend the system's nonlinear performance. Figure 3 depicts a simplified form of a single magnet active magnetic bearing. Here a 'U' shaped actuator is used with a disk shaped rotor having a mass m (Debnath & Biswas, 2021b). The air gap is denoted as x and the current in the coils of magnet is represented as i. The magnet's produced force F is a function of the air gap (x), and the current in the magnet coils (i).

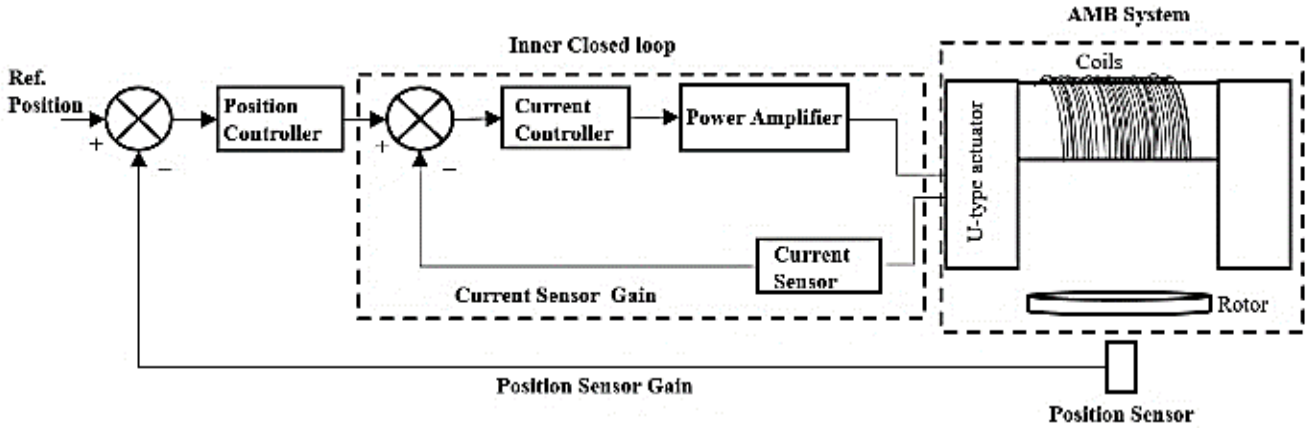

Figure 2. Proposed closed loop AMB system.

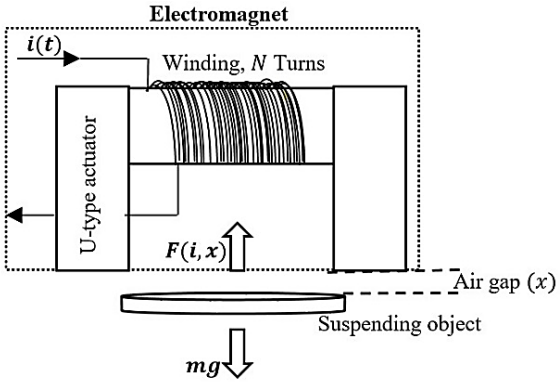

Figure 3. Simplified model of active magnetic bearing.

A. Mechanical dynamics modelling of the system

In terms of air gap, mechanical dynamics are

$$m\left(\frac{d^2x}{dt^2}\right) = mg - F(i,x) \tag{1}$$

Here, force F is attractive force of electromagnet which nonlinearly depends on two variables i and x.

B. Magnetic force modelling of the system

Rotor and stator are made of iron having permeability many times greater than the of air. The reluctance is,

$$R(x) = \frac{x}{\mu_o A} \tag{2}$$

where, μ_o = permeability of air= $4\pi \times 10^{-7} H/m$

Magnetic flux in terms of magneto motive force and effective reluctance,

$$\phi(i,x) = \frac{\mu_o A N i}{x} \tag{3}$$

therefore, flux linkage is,

$$\lambda(i,x) = N\phi = \frac{\mu_o A N^2 i}{x} \tag{4}$$

magnetic co-energy is,

$$W_c\,(i,x) = \int_0^i \lambda(i,x)dx \tag{5}$$

the connection between magnetic force and magnetic co-energy,

$$F = \frac{\partial W_C(i,x)}{\partial x} \tag{6}$$

using Eq. 4 and Eq. 5, the electromagnetic force is,

$$F(i,x) = -\frac{\mu_o A N^2}{2}\left(\frac{i}{x}\right)^2 \tag{7}$$

negative sign shows that the force applied by magnet is counteracting gravity on the rotor. So as magnetic force increases the rotor moves closer to the magnet.

Using Taylor's series expansion, Eq. 7 is linearized (Hurley & Wolfle, 1997) at an equilibrium point (i_o, x_o). In form of transfer function, it is given as,(Debnath & Biswas, 2020)

$$G(s) = \frac{X(s)}{I(s)} = \frac{\frac{C_a}{m}}{s^2 - \frac{C_z}{m}} \tag{8}$$

Eq. 8 shows the linearized AMB system transfer function relating coil in the current I(s) and air gap X(s). where C_z and C_a depends on plant parameters (Debnath & Biswas, 2021a).

Using Eq. 8 and plant parameters shown in Table 1, for equilibrium point of operation a transfer function is calculated as:

$$G(s) = \frac{X(s)}{I(s)} = \frac{7.69}{s^2 - 1877.49} \tag{9}$$

Table 1. Simulation model parameter of proposed AMB system.

S.N.	Parameter	Values	Unit
1.	Mass of rotor (m)	0.065456	Kg
2.	Resistance of the coil (R)	1.2	Ω
3.	Inductance of coil (L) at x_o airgap	0.020598	H
4.	C_a	0.5033	N/A
5.	C_z	122.8935	N/m
At equilibrium,			
1.	i_o	2.44	A
2.	x_o	0.01	m

3. Designing of controllers

3.1. Designing of PID controller

This section is focused on designing a PID as a position controller for the AMB system. The switching frequency of inner closed loop is very high as compared to the outer closed loop (He et al., 2020). So, as an assumption, for designing the controller for outer loop (i.e., position controller), the inner

loop is considered as unity gain. But for verification, the complete AMB system is observed with the designed controller and the impact of the inner loop on overall performance is studied.

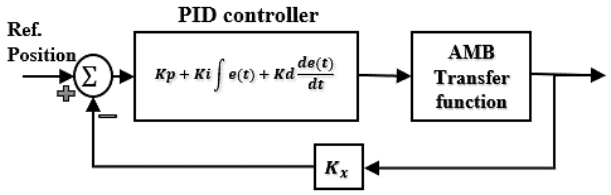

Figure 4. AMB system with a PID controller when inner closed loop is unity.

The PID controller transfer function $K(s)$,

$$K(s) = \frac{(sKp + Ki + s^2Kd)}{s} \tag{10}$$

where K_p= Proportional gain, K_i= Integral gain and K_d =Derivative gain. PID controller with AMB system as shown in Figure 4 can be write in equation form by using Eq. 8 and Eq. 10, then open loop transfer function will be,

$$G_{OL}(s) = G(s)H(s)$$

$$G_{OL}(s) = \frac{(sK_p + K_i + s^2K_d)}{s} * \frac{\frac{C_a}{m}}{s^2 - \frac{C_z}{m}} * K_x \tag{11}$$

where K_x = feedback path gain or, position sensor gain. For frequency response analysis (Katebi, 1988) the open loop transfer function after putting $s = j\omega$ will be,

$$G_{OL}(j\omega) = G(j\omega) * K(j\omega) * K_x$$

$$G_{OL}(j\omega) = \frac{K_xC_a(\omega^2K_d - K_i)}{m\left(\omega^2 + \frac{C_z}{m}\right)} \frac{\frac{(1 + j\omega)K_p}{(K_i - \omega^2K_d)}}{j\omega} \tag{12}$$

therefore,

$$\angle G(j\omega)H(j\omega) = \phi$$

$$\angle G(j\omega)H(j\omega) = 90° + tan^{-1}\left(\frac{\omega}{x - \omega^2 y}\right) \tag{13}$$

where, $x = K_i/K_p$ and $y = K_d/K_p$

at gain crossover frequency the magnitude of the open loop system is,

$$|G(j\omega)H(j\omega)| = 1$$

$$\frac{K_xC_a(\omega^2K_d - K_i)}{\omega(m\omega^2 + C_z)} \sqrt{1 + \frac{\omega^2K_p^2}{(K_i - \omega^2K_d^2)}} = 1 \tag{14}$$

so,

$$K_p = \frac{(m\omega^2 + C_z)cot\phi}{K_xC_a\sqrt{1 + co\,t^2\,\phi}} \tag{15}$$

Therefore,

$$y = \frac{\omega tan\phi - x}{\omega^2} \tag{16}$$

by using Eq. 13, Eq. 15, Eq. 16, x and y the calculated value of K_p, K_i and K_d for closed loop AMB system at equilibrium point of operation is 4.3, 184.2 and 0.052, respectively. Therefore, Eq. 10 becomes, a PID controller is simulated using operational amplifiers, resistors and capacitors which is depicted in Figure 11. Performance of this PID controller with proposed system is observed in later section of this manuscript.

$$K(s) = \frac{\left(4.3s + 184.2 + s^2(0.052)\right)}{s} \tag{17}$$

3.2. Designing of fuzzy logic controller (FLC)

Control of complex and uncertain systems was a major challenge until the introduction of fuzzy sets (Zadeh, 1988) and fuzzy control. These fuzzy sets along 'with if-and-then' statements, create an algorithm to control complicated systems. These if-and-then statements formed using qualitative process knowledge and human-like thinking (Zadeh, 1990). A block diagram representation of FLC is depicted in Figure 5.

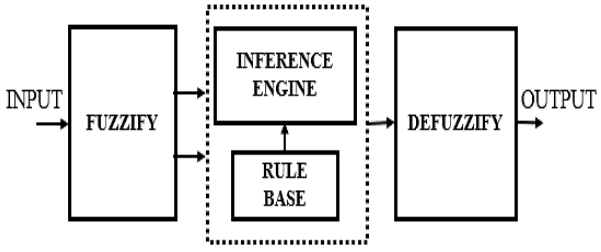

Figure 5. Block diagram of FLC.

Steps in designing fuzzy logic control technique are- Fuzzification, Inference and Defuzzification (Cox, 1992; Das & Biswas, 2021; Shieh, 2014). Each step has its own significance

which is briefly described and a two-dimensional FLC will be designed for the proposed AMB system.

A. Fuzzification

The first step after collecting all analogue data and crisp data is to transform it into the membership function of fuzzy subsets or, fuzzy sets. That it will be understandable by the inference system (Sain et al., 2020). Here, triangular type membership function converts the crisp data into fuzzy sets and subsets. Figure 6 shows a triangular membership function, and its mathematical description is given by Eq. 18.

$$\mu_A(x) = \begin{cases} 0, & if\ x \le -l \\ \dfrac{x-(-l)}{m-(-l)} & if\ -l < x \le m \\ \dfrac{l-x}{l-m}, & if\ m < x < l \\ 0, & if\ x \ge l \end{cases} \quad (18)$$

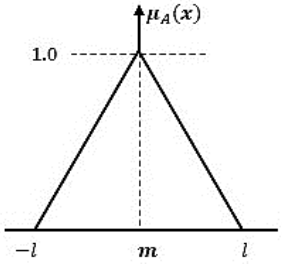

Figure 6. A triangular membership functions.

Here $\mu_A(x)$ is the value of membership function. The inputs are in range of $[-l, l]$, where m is a point having a magnitude of '1' and m lies in range of $-l \le m \le l$ (Das Sharma, 2012). The range is limited by the designer and depending upon the requirement the number of membership functions can be increased or decreased.

In this work the fuzzy controller employs two inputs: the error signal $e(t)$ (i.e., result of comparison between reference signal $r(t)$ and process output signal $y(t)$) and change in error signal $\frac{de(t)}{dt}$,as shown in Figure 7.

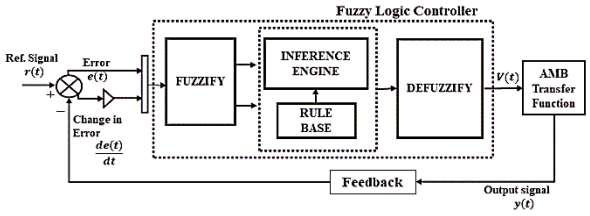

Figure 7. Closed loop AMB system with PD-fuzzy logic controller.

These two inputs, error signal $e(t)$ and change in error (i.e.,$\frac{de(t)}{dt}$) are ranged from [-1,1] and output voltage signal $\Delta V(t)$ is ranged from [-2,2]. Each input and output are fuzzified using seven symmetrical triangular type membership functions as depicted in Figure 8 (a) and (b). Here, $\mu_e(x) =$ membership function of error signal $e(t)$, $\mu_{\dot{e}}(x) =$ membership function of change in error signal $\frac{de(t)}{dt}$ and $\mu_V(x) =$ membership function of voltage $\Delta V(t)$.

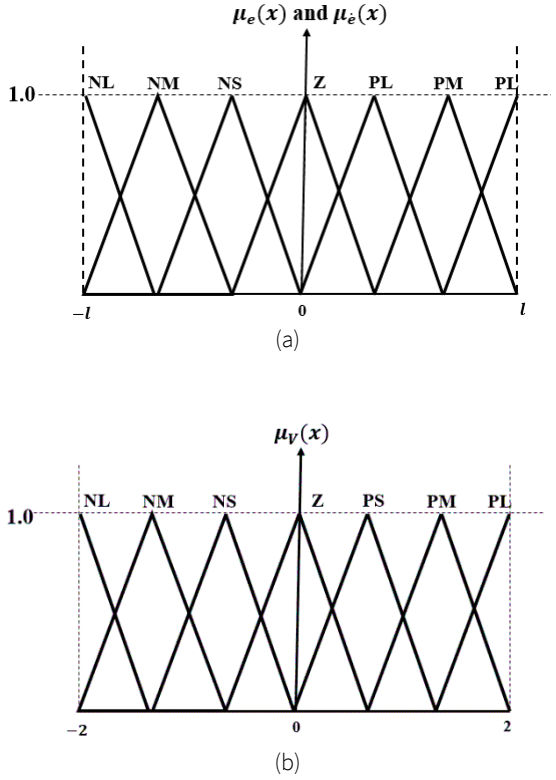

Figure 8. (a) Fuzzified inputs with seven triangular type membership function, (b) Fuzzified output with seven triangular type membership function.

Mathematically, $\mu_e(x)$, $\mu_{\dot{e}}(x)$ and $\mu_V(x)$ comprises of seven membership functions in their specific range (Agarwal & Chand, 2011). The terms NL, NM, NS, Z, PS, PM, and PL represent negative large, negative medium, negative small, zero, positive small, positive medium, and positive large respectively. The list of fuzzified input membership functions with their range is in Table 2 and output membership functions is listed in Table 3.

Table 2. Range of input membership functions.

Sl. No.	Membership functions of error signal	Membership functions of change in error signal	Range
1.	$\mu_{e_{NL}}(x)$	$\mu_{\dot{e}_{NL}}(x)$	$[-1,-0.6665]$
2.	$\mu_{e_{NM}}(x)$	$\mu_{\dot{e}_{NM}}(x)$	$[-1,-0.3334]$
3.	$\mu_{e_{NS}}(x)$	$\mu_{\dot{e}_{NS}}(x)$	$[-0.6665,0]$
4.	$\mu_{e_Z}(x)$	$\mu_{\dot{e}_Z}(x)$	$[-0.3334,0.3334]$
5.	$\mu_{e_{PS}}(x)$	$\mu_{\dot{e}_{PS}}(x)$	$[0,0.6665]$
6.	$\mu_{e_{PM}}(x)$	$\mu_{\dot{e}_{PM}}(x)$	$[0.3334,1]$
7.	$\mu_{e_{PL}}(x)$	$\mu_{\dot{e}_{PL}}(x)$	$[0.6665,1]$

Table 3. Range of output membership function.

Sl. No.	Membership functions of voltage signal	Range
1.	$\mu_{V_{NL}}(x)$	$[-2,-1.3334]$
2.	$\mu_{V_{NM}}(x)$	$[-2,-0.6668]$
3.	$\mu_{V_{NS}}(x)$	$[-1.3334,0]$
4.	$\mu_{V_Z}(x)$	$[-0.6668,0.6668]$
5.	$\mu_{V_{PS}}(x)$	$[0,1.3334]$
6.	$\mu_{V_{PM}}(x)$	$[0.6668,2]$
7.	$\mu_{V_{PL}}(x)$	$[1.3334,2]$

Later, depending upon the rule base, operation is performed on fuzzified inputs and output in the inference engine.

B. Inference and rule base

Fuzzy inference is the process of creating a map utilizing fuzzy logic from a given input to an output. Mapping then provides a basis for judgement and trend detection. Rule base describes the mapped relation between fuzzified inputs and output. In this work, if-and-then rule is designed using two different inputs and one output, with seven membership function each, i.e., $7^2 = 49$ rules relating to the inputs and output. Table 4. shows a rule base for designing FLC.

With reference to Table 4, all the rules can be stated in form of- "IF error is PL (positive large) AND change in error is NM (negative medium) THEN voltage is PS (positive small)". In terms of membership functions, it can be rewritten as- "IF error is $\mu_{e_{PL}}(x)$ AND change in error $\mu_{\dot{e}_{NM}}(x)$ THEN voltage is $\mu_{V_{PS}}(x)$".

Similarly, all the 49 rules are created in rule base editor of fuzzy tool of MATLAB. Depending upon these rules the inference engine executes the process and generates output accordingly (Li & Gatland, 1996). The output is further defuzzified (i.e., conversion of fuzzified data into raw data or crisp data) to make the output data understandable.

Table 4. Rule base.

$\dot{e}$ / e	PL	PM	PS	Z	NS	NM	NL
NL	Z	NS	NM	NL	NL	NL	NL
NM	PS	Z	NS	NM	NL	NL	NL
NS	PM	PS	Z	NS	NM	NL	NL
Z	PL	PM	PS	Z	NS	NM	NL
PS	PL	PL	PM	PS	Z	NS	NM
PM	PL	PL	PL	PM	PS	Z	NS
PL	PL	PL	PL	PL	PM	PS	Z

C. Defuzzification

There are more than seven methods are available for defuzzification purpose. All have their significances and advantages. But among them the most useful method is centroid method or, center of area method (Mohan & Sinha, 2008). Based on the center of gravity of the fuzzy set, this technique delivers an exact value. It can be defined by the algebraic expression, (Eq. 19). Pictorial representation of centroid method of defuzzification is shown in Figure 9.

$$x^* = \frac{\int x\,\mu_A(x)\,dx}{\int \mu_A(x)\,dx} \tag{19}$$

where, x^*= defuzzified value of x

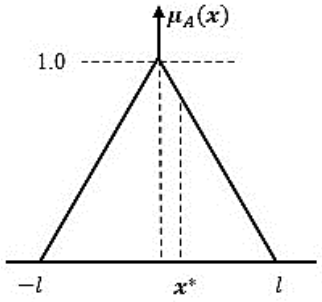

Figure 9. Centroid method of defuzzification.

3.2.1. Designing of proportional integral derivative-fuzzy logic controller (PID-FLC)

The designed FLC, shown in Figure 7 is a PD-FLC which can be modified to perform as a PID -FLC (Arun & Mohan 2018; Lai & Lin, 2003). Implementing an integrator to the output of PD-FLC and taking a summation of output of the integrator with output of PD-FLC becomes a PID-FLC (Li, 1997) as shown in Figure 10.

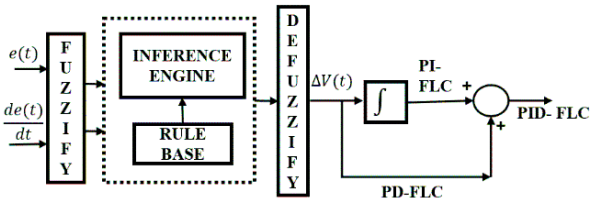

Figure 10. A simplified PID-Fuzzy logic controller (PID-FLC).

The designed PID-FLC is used as a position controller for the proposed AMB system, its performance is observed and compared with PD-FLC and PID controller. In the next section, different controllers will be simulated with the proposed AMB system, and their effect and performance are observed.

4. Simulation, results, and discussion

4.1. Simulation of proposed active magnetic bearing (AMB) system with PID controller

For different parts of PID controller resistor and capacitor values are calculated as:

For proportional part of PID controller when K_p=4.3,

$$K_p = \frac{R_p}{R_{in}} \tag{20}$$

let, R_{in} =1 $K\Omega$

$$R_p = \frac{1000}{4.3} = 232.2\ \Omega$$

for integral part of PID controller when K_i =184.2,

$$K\_i = \frac{1}{R_i C_i} \tag{21}$$

let, $C_i = 1 \times 10^{-6} F$

$$R_i = \frac{1}{184.2 \times 1 \times 10^{-6}} = 5428.88\ \Omega$$

for derivative part of PID controller when K_d =0.052,

$$K_d = R_{i1} C_{i1} \tag{22}$$

let, $C_{i1} = 1 \times 10^{-6} F$

$$R_{i1} = \frac{0.052}{1 \times 10^{-6}} = 52K\Omega$$

using these values of $R_p, R_{in}, R_i, C_i, R_{i1}$and C_{i1} a PID controller is simulated as shown in Figure 11. and a pulse of unit step is applied to it to observe output of each part of PID controller.

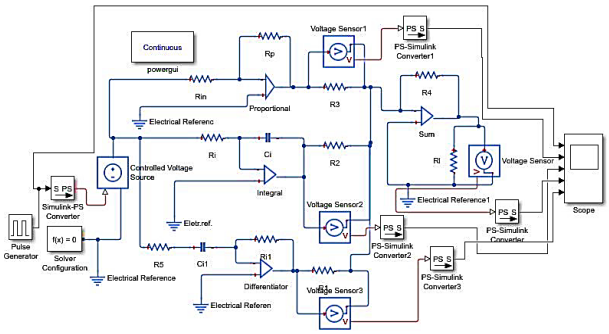

Figure 11. PID controller using analog electronics components is designed in Simulink MATLAB.

Figure 12 shows the input, which is a pulse of unit step signal for three cycles and output of each part of PID controller. (i.e., proportional, integral, and derivative respectively).

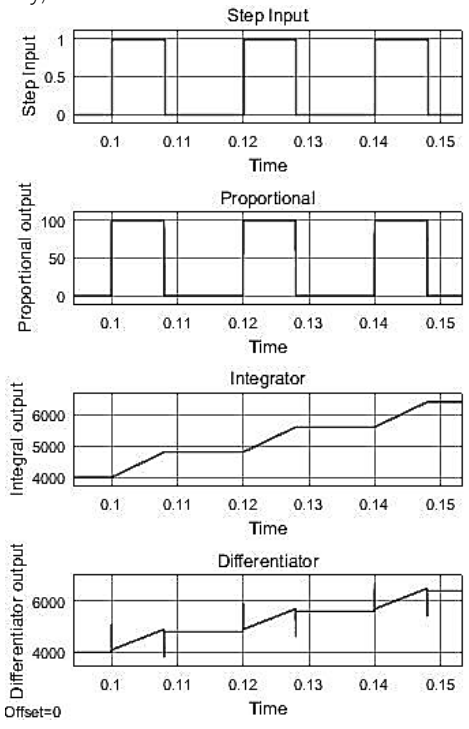

Figure 12. Output of different parts of PID controller for a pulse of unit step input signal.

In this study, transfer function (Eq. 9) is used for all observation and computation. With reference to Figure 4, when the inner closed loop is set to unity, the proposed AMB system is simulated with a PID controller, as illustrated in Figure 13.

A unit step signal is provided as input to the system, allowing observers to examine how the closed loop performs in transient state.

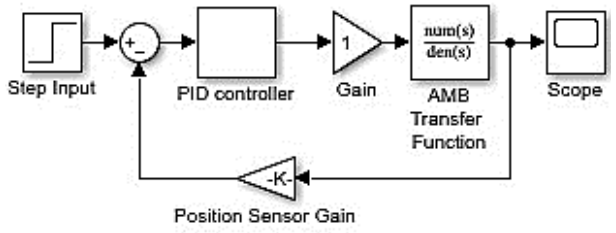

Figure 13. Proposed AMB system
(when inner closed loop is unity) with PID controller.

Observed transient state parameters are listed in Table 8, where percentage overshoot is 18.452% which is in a stable region at the peak time is 0.066 sec, rise time is 0.02468 sec and settling time is 0.14287 sec. Calculated damping ratio (ξ)= 0.47268, which is in between control design limit that is $0< \xi <1$.

Next, the complete proposed AMB system, as depicted in Figure 2, is simulated. Here, the current controller is a Proportional-Integral (PI) (He et al., 2020), and a single switch power amplifier (Debnath et al., 2020) is intimated for the inner closed loop. The designed PID controller is implemented as a position controller. The simulation layout of the complete AMB system is shown in Figure 14, and for a unit step signal, step response has been plotted and transient state parameters have been observed which are listed in Table 8.

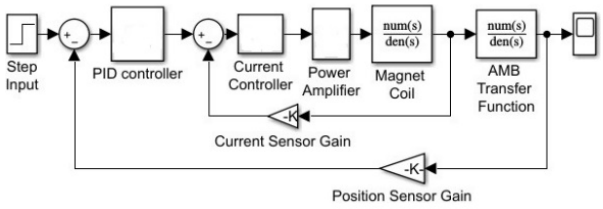

Figure 14. Complete AMB system with PID controller.

Transient response of complete proposed AMB system is studied which has a peak overshoot of 22.84% at a peak time of 0.070 sec, rise time is 0.02637 sec, settling time is 0.14164 sec and calculated damping ratio (ξ) = 0.4253.

To compare the transient state performances of both forms of the closed loop with the designed PID controller, step responses are plotted on an X-Y axis as shown in Figure 15. It is evident from the step plots of Figure 15 that the designed PID controller when implemented with the complete proposed AMB system shows a rise in overshoot, rise time and peak time. This change in transient state parameters (which is listed in Table 5) is due to the presence of an inner closed loop. Although, the designed PID controller is still able to maintain the system in underdamped region $(0 < \xi < 1)$.

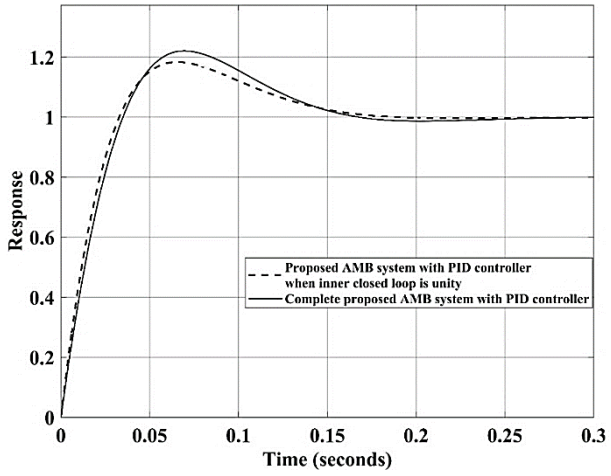

Figure 15. Step responses with PID controller.

Table 5. Change in transient state parameters with PID controller.

Transient state parameters	Change in value
Percentage Overshoot	+23.78%
Peak Time	+6.060%
Damping Ratio (ξ)	-10.00%
Rise Time	+6.875%
Settling Time	-0.860%

Using the designed PID controller with complete proposed AMB system the percentage overshot increased by 23.78% and damping ratio reduced by 10%. There is a little decrement in the settling time which means that the complete proposed AMB system with PID controller settles fast as compared to proposed AMB system with PID controller (when inner closed loop is unity).

4.2. Simulation of proposed active magnetic bearing (AMB) system with PD-FLC

Fuzzy logic controller (FLC) is designed for the proposed system using fuzzy toolbox application of MATLAB (The MathWorks, 1998). For creating a fuzzy rule base, the first crisp data input and output has been defined in a form of membership function as shown in Figure 16 (a) and (b). Later this fuzzified data is processed to an inference engine and depending upon the designed rules output is generated which is defuzzified into crisp data form.

In this paper, fuzzy inference system (FIS) is of Mamdani type (Aceves-López & Aguilar-Martin, 2006) and rule base editor creates all of the 49 rules which has been described in subsection 3.2. A three-dimensional plot of rule base is shown

in Figure 17 where on X-axis error signal is labelled, change in error signal is labelled on Y-axis and output is laid out on Z-axis, to their respective range.

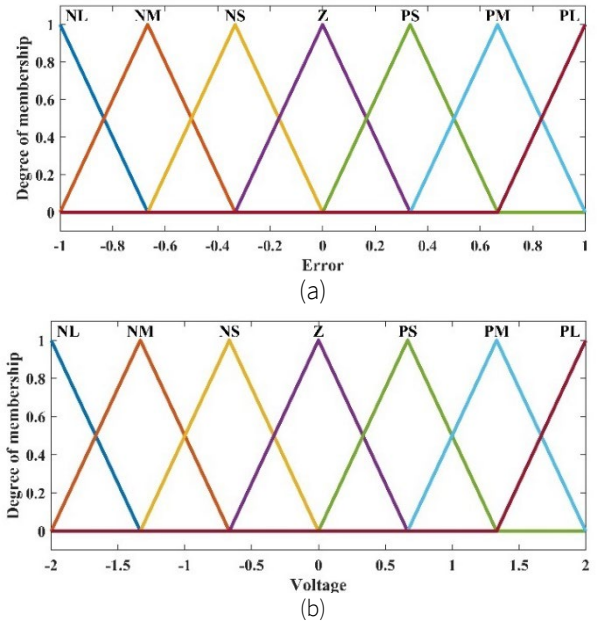

Figure 16. (a) Fuzzified inputs and (b) Fuzzified output with seven triangular type membership function.

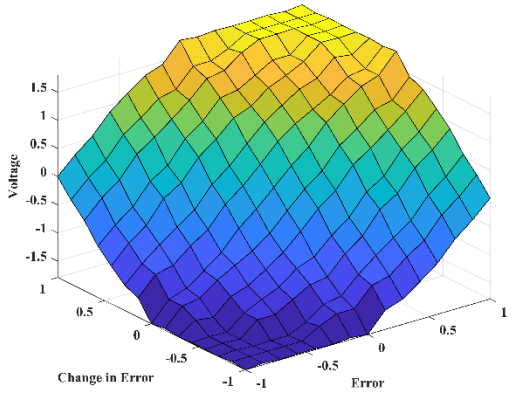

Figure 17. Three-dimensional plot of fuzzy rules.

As illustrated in Figure 18, the created fuzzy logic controller is also employed as a position controller with the proposed AMB system.

When PD-FLC is a position controller for the proposed AMB system (when inner closed loop is unity) shows a peak overshoot of 8.152% which is 10.3 unit less than PID controlled. With the implementation of PD-FLC as a position controller, rise time, peak time and settling time of the closed loop reduce to 19.327%, 30.30% and 34.457% respectively (compared to PID controller).

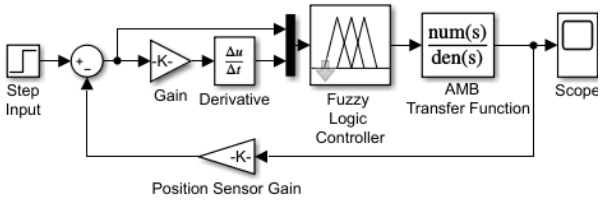

Figure 18. Proposed AMB system (when inner closed loop is unity) with PD-FLC.

Referring to Figure 2, the complete proposed AMB system is simulated in MATLAB with PD-FLC as a position controller as shown in Figure 19.

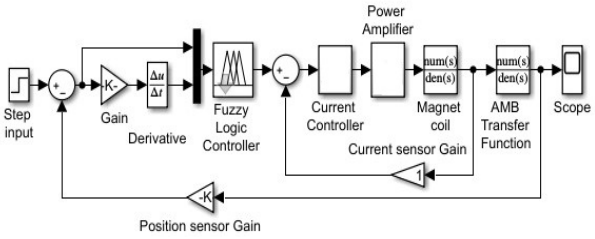

Figure 19. Complete proposed AMB system with PD-Fuzzy logic controller (PD-FLC).

Comparing the data obtained for PD-FLC with complete proposed AMB system, with PID controller, shows a reduction of 58.96% in peak overshoot with a value of 14.368%, other than this peak time, rise time and settling time also get reduced by 42.85%, 36.67% and 27.32% respectively.

Due to the inner closed loop, the peak overshoot value for complete proposed AMB system with PD-FLC has increased but it is still 37.09% less than PID controller with complete proposed AMB system. The increment and decrement of various transient state parameters values of proposed AMB system (when inner closed loop is unity) and complete proposed AMB system with PD-FLC is listed in Table 6. Step responses for both forms of closed loop proposed AMB system is shown in Figure 20.

Reduction in rise time and peak time lead to a faster response but increased settling time make the complete system sluggish in steady state region but compared to PID controller with complete proposed AMB system, the performance is improved. Further improvement in transient state parameters can be observed with the implementation of PID-FLC as a position controller for the proposed system.

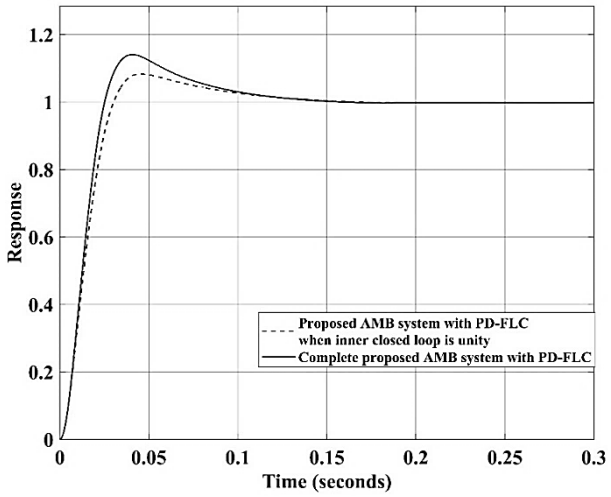

Figure 20. Step response with PD-FLC.

Table 6. Change in transient state parameters with PD-FLC.

Transient state parameters	Change in value
Percentage Overshoot	+76.25%
Peak Time	-13.0434%
Damping Ratio (ξ)	-15.757%
Rise Time	-16.122%
Settling Time	+9.9316%

4.3. Simulation of proposed active magnetic bearing (AMB) system with PID-fuzzy logic controller (PID-FLC)

PID-FLC as a position controller for the proposed AMB system (when inner closed loop is unity) is simulated in MATLAB as illustrated in Figure 21 and unit step signal is input to observe the step response of the closed loop.

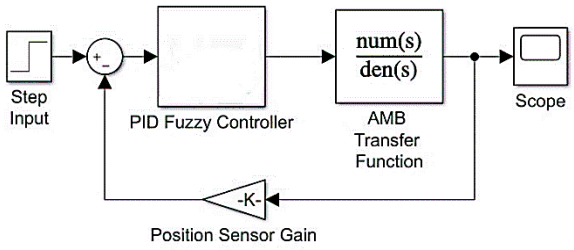

Figure 21. Proposed AMB system (when inner closed loop is unity) with PID-FLC.

Transient state parameters obtained by the step response of PID-FLC with proposed AMB system (when inner closed loop is unity) shows a decrement in peak overshoot. As compared to PID controller and PD-FLC, the peak overshot reduced by 62.12% and 14.266% respectively. Remaining other parameters like rise time, peak time and settling time also get reduced and their values are listed in Table 8, which makes the closed loop faster with less oscillations. The same PID-FLC is simulated with the complete proposed AMB system by applying a unit step signal as a reference signal which is shown in Figure 22.

The step response of complete proposed AMB system and proposed AMB system (when inner closed loop is unity) with PID-FLC is plotted in Figure 23 and changed data is shown in Table 7.

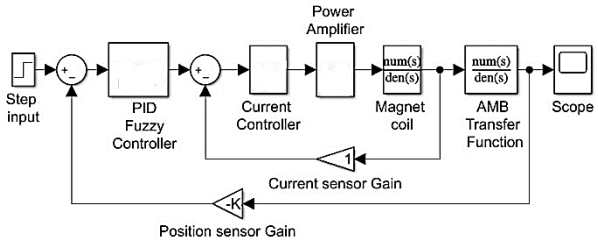

Figure 22. Complete proposed AMB system with PD-Fuzzy logic controller (PD-FLC).

The information in Table 8 makes it clear that the proposed AMB system with PID-peak FLC has an overshoot value of 11.798%. It is still the minimum obtained overshot as compared by PID controller and PD-FLC with complete proposed AMB system.

It is noticeable from Table 8 that implementing the PID-FLC on the complete proposed AMB system improves the overall response of the system.

Table 7. Change in transient state parameters with PID-FLC.

Transient state parameters	Change in value
Percentage Overshoot	+68.808%
Peak Time	-10.256%
Damping Ratio (ξ)	-12.969%
Rise Time	-7.83%
Settling Time	-10.946%

Next section will show comparison among performance of PID, PD-FLC and PID-FLC, as a position controller. First, with the proposed AMB system (when inner closed loop is unity) and then with the complete proposed AMB system.

4.4. Performance comparison among PID controller, PD-FLC and PID-FLC

For the proposed AMB system when inner closed loop is unity, the step responses with different controllers are shown in Figure 24 and data of the transient state parameters are listed in Table 8. Comparing the transient parameters values of PID controller with PID-FLC clears that the peak overshoot, rise time, peak time and settling time are improved by 62.12%, 32.21%, 40.90% and 58.88% respectively. This improvement

makes the closed loop faster and more robust to sudden changes.

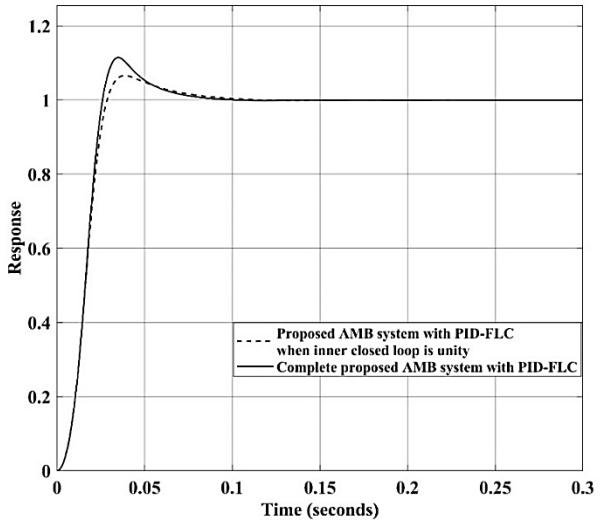

Figure 23. Step response with PID-FLC.

For second-order systems, the closed-loop damping ratio is (Nise, 2011),

$$\text{Phase margin} \cong 100 \times \text{damping ratio } (\xi) \quad (23)$$

Therefore, when inner closed loop is unity the Phase margin with PID controller ≅ 100 × 0.47268 = 47.26°, with PD-FLC ≅ 100 × 0.62372 = 62.372° and with PID-FLC ≅ 100 × 0.64630 = 64.630°.

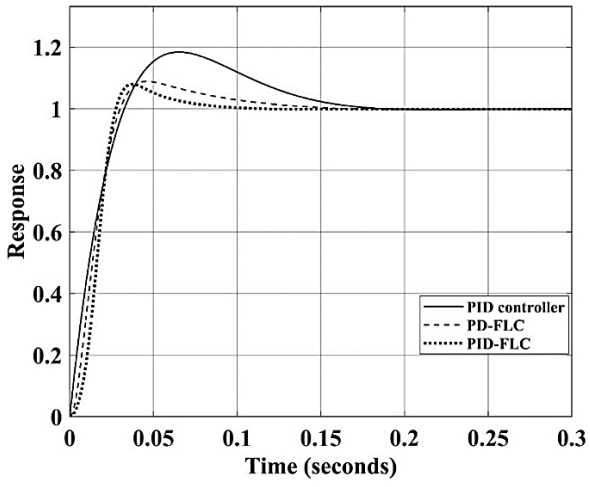

Figure 24. Step responses of proposed AMB system (when inner closed loop is unity) with PID controller, PD-FLC and PID-FLC.

Phase margin of a system shows allowable open loop phase change to a system to make its closed loop unstable. This margin should be so appropriate and precise as higher value of phase margin leads to a sluggish performance and lower value will show a little stability margin. With PID-FLC the phase margin of the system increased by 36.73% over PID which results in an increased stability region.

From Figure 24 it is noticeable that the PID-FLC gives a smooth and better transient performance as compared to PID and PD-FLC.

The step responses of different controllers with the complete proposed AMB system are depicted in Figure 25 and the related transient state parameters are shown in Table 8. Here, again the PID-FLC shows an improvement in performance over PID and PD-FLC and comparison between PID and PID-FLC explains that peak overshoot, rise time, peak time and settling time reduced by 48.345%, 41.52%, 50% and 49.18% respectively.

The phase margin of the complete proposed system with PID controller is 42.53°, with PD-FLC is 52.54° and with PID-FLC is 56.24°. The increased phase margin with PID-FLC (13.71° as compared to PID, almost 32.23% increment) represents that the complete proposed AMB system with PID-FLC is more stable as compared to PID and PD-FLC. Range of the dynamic parameters obtained from the analysis are listed in Table 9 below.

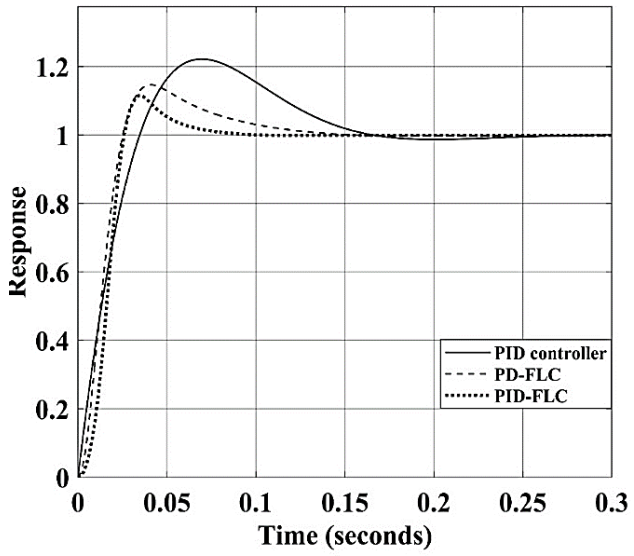

Figure 25. Step responses of complete proposed AMB system with PID controller, PD-FLC and PID-FLC.

Table 8. Transient state parameters with PID controller, PD-FLC and PID-FLC.

Proposed AMB System	When inner closed loop is unity			Complete proposed active magnetic bearing (AMB) system		
Type of Controller	PID controller	PD Fuzzy logic controller	PID Fuzzy logic controller	PID controller	PD Fuzzy logic controller	PID Fuzzy logic controller
Percentage Overshoot (%)	18.452	8.152	6.989	22.840	14.368	11.798
Peak Time (seconds)	0.066	0.046	0.039	0.070	0.040	0.035
Damping Ratio (ξ)	0.47268	0.62372	0.64630	0.42538	0.52544	0.56248
Rise Time (seconds)	0.02468	0.01991	0.01673	0.02637	0.01670	0.01542
Settling Time (seconds)	0.14287	0.09364	0.05874	0.14164	0.10294	0.05231
Steady State Error	0.001	0.001	0.001	0.001	0.001	0.001
Phase Margin (Degree)	47.268	62.372	64.63	42.538	52.544	56.248

Table 9. Range of dynamic parameters.

Sl. No.	Parameter	Range
1.	Percentage Overshoot (%)	6% to 23%
2.	Damping ratio (ξ)	0.40 to 0.65
3.	Peak Time (sec)	0.39 to 0.07
4.	Rise Time (sec)	0.015 to 0.027
5.	Settling Time (sec)	0.05 to 0.15
6.	Phase margin (Degree)	40^0 to 65^0

Table 10. Comparative analysis of proposed controller with available controllers.

Sl. No.	Controller used	Obtained Parameters values	Remarks	Ref. No.
1.	Lead	$\%M_P \approx 16$	One of the classical controllers which has three tuning parameters- pole, zero and gain. For 10mm air gap value the lead controller shows a peak overshoot of almost 16%	(Debnath & Biswas, 2020)
2.	PID	$\%M_p \approx 14$	A traditional PID controller with three tuning parameters- K_p, K_I and K_D	(Gupta et al., 2018)
3.	PID	$\%M_p$ is slightly greater than 15%	A performance comparison is conducted among a conventional PID, an incomplete differential PID and a PSO optimized fuzzy PID controller. Further observation is made by considering external disturbance.	(Bo et al., 2021)
	Incomplete PID	$\%M_p$ is slightly less than 15%		
	PSO-Fuzzy PID	$\%M_p$ is almost 11%		
4.	Integer order PID FO-PID	$\%M_p$ is almost 12% $\%M_p$ is almost 12%	Control performance compassion is observed for three set of integer order PID and a FO- PID controller for a radial four DOF active magnetic system.	(Zhang et al., 2021)

From Figure 24 it is noticeable that the PID-FLC gives a smooth and better transient performance as compared to PID and PD-FLC

The step responses of different controllers with the complete proposed AMB system are depicted in Figure 25 and the related transient state parameters are shown in Table 8. Here, again the PID-FLC shows an improvement in performance over PID and PD-FLC and comparison between PID and PID-FLC explains that peak overshoot, rise time, peak time and settling time reduced by 48.345%, 41.52%, 50% and 49.18% respectively.

The phase margin of the complete proposed system with PID controller is 42.53°, with PD-FLC is 52.54° and with PID-FLC is 56.24°. The increased phase margin with PID-FLC (13.71° as compared to PID, almost 32.23% increment) represents that the complete proposed AMB system with PID-FLC is more stable as compared to PID and PD-FLC. Range of the dynamic parameters obtained from the analysis are listed in Table 9 below.

Here, from the Table 9, it is easily observable that the phase margin for the overall system varies from 40^0 to 65^0. This range is most desirable as the system shows better stability and a speedy performance in between this range.

4.5. Comparative analysis

Peak overshoot is shown in the Table 10 above as $\%M_P$. Different academics have suggested a variety of controlling approaches for distinct structures and models of AMB system. It can be seen from Table 10, that there is a larger overshoot when using traditional controls like lead and PID. As modern or intelligent controllers like fuzzy, optimization techniques and FO-PID are implemented, the overall system performance gets improved. The minimum overshoot recorded with traditional controllers is 14% (nearly), while the minimum overshoot observed with fractional order-PID is 11%.

This overshoot is further enhanced with its related time domain parameters using fuzzy-PID controller. For the case when inner current controlling loop is unity, the fuzzy-PID controller shows a peak overshot of 6.989%. Considering the completely proposed loop of AMB system the obtained peak overshoot further reduces to 11.798%.

5. Conclusion

Active magnetic bearing (AMB) system is inherently nonlinear and open loop unstable system. Due to which, the proposed AMB system is first dynamically modelled and linearized at an equilibrium operating point (x_o, i_o). Then for proper bearing operation the proposed AMB system is described with its two closed loops. In this work, different position controllers for the proposed system are designed, simulated, and compared, these position controllers are conventional PID controller, proportional derivative-fuzzy logic controller (PD-FLC) and proportional integral derivative-fuzzy logic controller (PID-FLC).

It is evident from the data listed in Table 8 that PID-FLC gives overall a better transient state and steady state response as compared to PID and PD-FLC. Peak overshoot of the proposed AMB system (when inner loop is unity) reduces from 18.452% to 6.989% and the phase margin get increased by 36.731%, which increases the relative stability region of the system, remaining transient state parameters also get improved using PID-FLC. When rotor position of complete proposed AMB system is controlled by PID-FLC, reduces the overshoot by 48.345%, increases the speed (rise time) of the system by 41.52% and the system reaches to steady state 49.18% faster, as compared to PID controller.

Relative stability of the completely proposed AMB system (with PID-FLC) increases by a factor of 32.23% as compared to PID controller and 3.62% as compared to PD-FLC. Therefore, the observed data states that, the designed fuzzy logic-based controllers are managed to handle the instability of the proposed system much better than the conventional PID controller and can be further modified to improve the system performance

Conflict of interest

The authors have no conflict of interest to declare.

Funding

The authors received no specific funding for this work.

References

Aceves-López, A., & Aguilar-Martin, J. (2006). A simplified version of mamdani's fuzzy controller: the natural logic controller. *IEEE Transactions on fuzzy systems*, *14*(1), 16-30. https://doi.org/10.1109/TFUZZ.2005.861603

Agarwal, P. K., & Chand, S. (2011). Fuzzy logic control of three-pole active magnetic bearing system. *International Journal of Modelling, Identification and Control*, *12*(4), 395-411. https://doi.org/10.1504/IJMIC.2011.040083

Anantachaisilp, P., & Lin, Z. (2013). An experimental study on PID tuning methods for active magnetic bearing systems. *International Journal of Advanced Mechatronic Systems*, *5*(2), 146-154. https://doi.org/10.1504/IJAMECHS.2013.055991

Arun, N. K., & Mohan, B. M. (2018). Modelling, stability analysis and computational aspects of nonlinear fuzzy PID controllers using Mamdani minimum inference. *International Journal of Automation and Control*, *12*(1), 153-174. https://doi.org/10.1504/IJAAC.2018.088601

Bachovchin, K. D., Hoburg, J. F., & Post, R. F. (2012). Stable levitation of a passive magnetic bearing. *IEEE Transactions on Magnetics*, *49*(1), 609-617. https://doi.org/10.1109/TMAG.2012.2209123

Bachovchin, K. D., Hoburg, J. F., & Post, R. F. (2012). Magnetic fields and forces in permanent magnet levitated bearings. *IEEE Transactions on Magnetics*, *48*(7), 2112-2120. https://doi.org/10.1109/TMAG.2012.2188140

Bai, J. G., Zhang, X. Z., & Wang, L. M. (2012). A flywheel energy storage system with active magnetic bearings. *Energy Procedia*, *16*, 1124-1128. https://doi.org/10.1016/j.egypro.2012.01.179

Bangcheng, H., Shiqiang, Z., Xi, W., & Qian, Y. (2011). Integral design and analysis of passive magnetic bearing and active radial magnetic bearing for agile satellite application. *IEEE Transactions on Magnetics*, *48*(6), 1959-1966. https://doi.org/10.1109/TMAG.2011.2180731

Bassani, R. (2006). Earnshaw (1805–1888) and passive magnetic levitation. *Meccanica*, *41*, 375-389. https://doi.org/10.1007/s11012-005-4503-x

Bo, W., Haipeng, G., Hao, L., & Wei, Z. (2021). Particle swarm optimization-based fuzzy PID controller for stable control of active magnetic bearing system. In *Journal of Physics: Conference Series* (Vol. 1888, No. 1, p. 012022). IOP Publishing. https://doi.org/10.1088/1742-6596/1888/1/012022

Cox, E. (1992). Fuzzy Fundamentals. *IEEE Spectrum* 29 (10), 58–61. https://doi.org/10.1109/6.158640

Das, U., & Biswas, P. K. (2021). Relative study of classical and fuzzy logic controllers in a closed-loop BLDC motor drive with the GA and PSO optimization technique. *Journal of applied research and technology*, *19*(4), 379-402. https://doi.org/10.22201/icat.24486736e.2021.19.4.1039

Das Sharma, K. (2012). A systematic design methodology of PD fuzzy logic controller using cellular fuzzy logic concept. *International journal of Automation and Control*, *6*(3-4), 231-245. https://doi.org/10.1504/IJAAC.2012.051882

Debnath, S., & Biswas, P. K. (2021a). Study and analysis on some design aspects in single and multi-axis active magnetic bearings (AMB). *Journal of applied research and technology*, *19*(5), 448-471. https://doi.org/10.22201/icat.24486736e.2021.19.5.1211

Debnath, S., & Biswas, P. K. (2021b). Design, analysis, and testing of I-type electromagnetic actuator used in single-coil active magnetic bearing. *Electrical Engineering*, *103*(1), 183-194. https://doi.org/10.1007/s00202-020-01071-x

Debnath, S., & Biswas, P. K. (2020). Advanced magnetic bearing device for high-speed applications with an I-type electromagnet. *Electric Power Components and Systems*, *48*(16-17), 1862-1874. https://doi.org/10.1080/15325008.2021.1908454

Debnath, S., Biswas, P. K., & Das, U. (2018). Analysis and Simulation of Different Types of Power Amplifiers Used in Electromagnetic Levitation System. Journal of Power Technologies, 98(2).

Debnath, S., Biswas, P. K., & Laldingliana, J. (2020). Analysis, Simulation and Hardware Implementation of Single Switch Power Amplifier for Active Magnetic Bearing (AMB) system. Journal of Power Technologies, 100(4), 308.

Du, H., Zhang, N., Ji, J. C., & Gao, W. (2010). Robust fuzzy control of an active magnetic bearing subject to voltage saturation. *IEEE transactions on control systems technology*, *18*(1), 164-169. https://doi.org/10.1109/TCST.2008.2009644

Gupta, S., Laldingliana, J., Debnath, S., & Biswas, P. K. (2018). Closed loop control of active magnetic bearing using PID controller. In *2018 International Conference on Computing, Power and Communication Technologies (GUCON)* (pp. 686-690). IEEE. https://doi.org/10.1109/GUCON.2018.8675123

He, Y., He, X., Ma, J., & Fang, Y. (2020). Optimization research on a switching power amplifier and a current control strategy of active magnetic bearing. *IEEE Access*, *8*, 34833-34841. https://doi.org/10.1109/ACCESS.2020.2974765

Hong, S. K., & Langari, R. (2000). Robust fuzzy control of a magnetic bearing system subject to harmonic disturbances. *IEEE Transactions on Control Systems Technology*, *8*(2), 366-371. https://doi.org/10.1109/87.826808

Hoshi, H., Shinshi, T., & Takatani, S. (2006). Third-generation blood pumps with mechanical noncontact magnetic bearings. *Artificial organs*, *30*(5), 324-338. https://doi.org/10.1111/j.1525-1594.2006.00222.x

Hung, J. Y. (1995). Magnetic bearing control using fuzzy logic. *IEEE Transactions on Industry Applications*, *31*(6), 1492-1497. https://doi.org/10.1109/28.475746

Hurley, W. G., & Wolfle, W. H. (1997). Electromagnetic design of a magnetic suspension system. *IEEE Transactions on education*, *40*(2), 124-130. https://doi.org/10.1109/13.572325

Imai, S., & Yamamoto, T. (2012). Design of a multiple linear models-based PID controller. *International Journal of Advanced Mechatronic Systems*, *4*(3-4), 141-148. https://doi.org/10.1504/IJAMECHS.2012.051575

Jiang, D., Li, T., Hu, Z., & Sun, H. (2020). Novel topologies of power electronics converter as active magnetic bearing drive. *IEEE Transactions on Industrial Electronics,* 8(2), 950-959. https://doi.org/10.1109/ACCESS.2020.2974765

Katebi, S. D. (1988). *Control systems engineering*, IJ Nagrath and M. Gopal, 725 pp, PBK, Wiley Eastern, 1982 https://doi.org/10.1002/acs.4480020212

Lai, Y. S., & Lin, J. C. (2003). New hybrid fuzzy controller for direct torque control induction motor drives. *IEEE Transactions on Power Electronics*, *18*(5), 1211-1219. https://doi.org/10.1109/TPEL.2003.816193

Li, H. X. (1997). A comparative design and tuning for conventional fuzzy control. *IEEE Transactions on Systems, Man, and Cybernetics, Part B (Cybernetics)*, *27*(5), 884-889. https://doi.org/10.1109/3477.623242

Li, H. X., & Gatland, H. (1996). Conventional fuzzy control and its enhancement. *IEEE Transactions on Systems, Man, and Cybernetics, Part B (Cybernetics)*, *26*(5), 791-797. https://doi.org/10.1109/3477.537321

Mohan, B. M., & Sinha, A. (2008). The simplest fuzzy two-term controllers: mathematical models and stability analysis. *International Journal of Automation and Control*, *2*(1), 5-21. https://doi.org/10.1504/IJAAC.2008.020426

Mushi, S. E., Lin, Z., & Allaire, P. E. (2012). Design, construction, and modeling of a flexible rotor active magnetic bearing test rig. *IEEE/ASME transactions on mechatronics*, *17*(6), 1170-1182. https://doi.org/10.1109/TMECH.2011.2160456

Nise, N. S. (2011). Control system engineering, john wiley & sons. Inc, New York.

Polajžer, B., Ritonja, J., Štumberger, G., Dolinar, D., & Lecointe, J. P. (2006). Decentralized PI/PD position control for active magnetic bearings. *Electrical Engineering*, *89*, 53-59. https://doi.org/10.1007/s00202-005-0315-1

Raj, R., & Mohan, B. M. (2020). Takagi-Sugeno fuzzy PID controllers: mathematical models and stability analysis with multiple fuzzy sets. *International Journal of Fuzzy Computation and Modelling*, *3*(1), 33-60. https://doi.org/10.1504/ijfcm.2020.106093

Sain, C., Banerjee, A., Biswas, P. K., & Balas, V. E. (2020). Performance optimisation for closed loop control strategies towards simplified model of a PMSM drive by comparing with different classical and fuzzy intelligent controllers. *International Journal of Automation and Control*, *14*(4), 469-493. https://doi.org/10.1504/IJAAC.2020.108281

Schweitzer, G., Bleuler, H., & Traxler, A. (1994). Basics, properties and applications of active magnetic bearings. Active Magnetic Bearings, 210, 1-112.

Shieh, C. S. (2014). Segmented control based on fuzzy logic control for non-linear inverted pendulum swing-up. *International Journal of Automation and Control*, *8*(1), 88-97. https://doi.org/10.1504/IJAAC.2014.061666

Schweitzer, G. (2005). Safety and Reliability Aspects for Active Magnetic Bearing Applications - A Survey. Proceedings of the Institution of Mechanical Engineers, *Part I: Journal of Systems and Control Engineering*. *219*(6), 383-392. https://doi.org/doi:10.1243/095965105X33491

Schweitzer, G., & Maslen, E. H. (2009). *Magnetic Bearings: Theory, Design, and Application to Rotating Machinery*. Vol. 1. Springer Berlin. https://doi.org/10.1007/978-3-642-00497-1

The MathWorks, Inc. (1998). *Fuzzy Logic Toolbox: for Use with MATLAB: User's Guide*. Mathworks, Incorporated. https://in.mathworks.com/products/fuzzy-logic.html

Wang, Q. G., Lee, T. H., Fung, H. W., Bi, Q., & Zhang, Y. (1999). PID tuning for improved performance. *IEEE Transactions on control systems technology*, *7*(4), 457-465. https://doi.org/10.1109/87.772161

Yordanova, S. (2009). A frequency domain design of robust fuzzy PI controller for industrial processes. *International Journal of Automation and Control*, *3*(1), 4-25. https://doi.org/10.1504/IJAAC.2009.023068

Zadeh, L A. 1988. "Fuzzy Logic." *Computer* 21 (4): 83–93. https://doi.org/10.1109/2.53

Zadeh, L. A. (1990). The birth and evolution of fuzzy logic. *International Journal of General System*, *17*(2-3), 95-105. https://doi.org/10.1080/03081079008935102

Zhang, X., Bao, H., Du, J., & Wang, C. (2014). Application of a new membership function in nonlinear fuzzy PID controllers with variable gains. *Journal of Applied Mathematics*, *2014*. https://doi.org/10.1155/2014/482489

Zhang, Z., Xiong, H., & He, C. (2021). Research on Active Magnetic Bearing Rotor System Based on Fractional PID Control. In *2021 6th Asia Conference on Power and Electrical Engineering (ACPEE)* (pp. 868-872). IEEE. https://doi.org/10.1109/ACPEE51499.2021.9436868